J Electroceram (2006) 16:495–498
DOI 10.1007/s10832-006-9904-2

Calculation of the intrinsic dead layers thicknesses from Au/$Ba_{0.5}Sr_{0.5}TiO_3$/Pt thin film capacitors

Jooyoung Kim · Jaemoon Pak · Kuangwoo Nam · Gwangseo Park

Abstract Ferroelectric $Ba_{0.5}Sr_{0.5}TiO_3$ (BST) films were prepared on Pt/Ti/SiO_2/Si substrates by the sol-gel process. The films were spin-coated at 2000 rpm for 30 secs and then pyrolysed for 5 mins at the temperature of 350°C. This coating procedure was repeated for 3, 4, 5 and 6 times to obtain BST films with different thicknesses. After coating the films with the desired repetition times, the films were finally annealed in a conventional furnace at temperatures ranging from 600°C to 800°C with a 50°C interval in between. The films obtained with an annealing procedure of 750°C were polycrystalline with the presence of an impurity $BaCO_3$ phase. The capacitance and leakage current were measured and used to extract information on the metal-BST interface. With the series capacitance model and modified Schottky emission equation, the thickness of the dead layers for Au/BST and Pt/BST interfaces were calculated to be less than 6 nm and 5 nm, respectively.

Keywords Ferroelectric · Dead layers · (Ba, Sr)TiO_3

1 Introduction

Ferroelectric materials are of great technological impotance as promising candidates in a wide range of applications due to their unique properties of having two polarization states. Applications of ferroelectric devices includes dynamic random access memories (DRAM) [1], nonvolatile ferroelectric memories [2, 3], microwave tunable phase shifters [4, 5], electro-optical modulators and second harmonic generators [6]. High dielectric constant (Ba,Sr)TiO_3 (BST), a ferroelectric that shows strict paraelectric property is a promising material under intense investigation to be used as a dielectric layer in high-density DRAM as well as decoupling capacitors in monolithic microwave integrated circuits [7, 8].

Bulk BST was reported to have a dielectric constant (ε_r) value to be greater than 1000 [9]. However, when thin BST films is being produced, a common problem involving the decrease of dielectric constant with respect to film thickness is still an unsolved problem [10]. At present, there are assumptions that such phenomenon is caused by the presence of an intrinsic dead layer [11], defects leading to electrode polarization [12], and film stress from the substrate [13]. Thus, accurately quantifying the characteristics such as the thickness dependence of the dielectric constant in the ferroelectric film and understanding its origin is an important task to be solved before practical applications.

Intrinsic dead layer is the most widely accepted explanation, assuming that a severely depressed dielectric constant layers at the film/electrode interface is present, it forms a parasitic capacitor in series with the "bulk-like" ferroelectric layer. Hence, the decrease in dielectric constant is said to follow the "series capacitor model" [14]. As ferroelectric films between conventional metal electrodes are commonly used during integrating on silicon, multilayered platinized silicon substrates (Pt/Ti/SiO_2/Si) is mostly favored, with advantages of having good stability in high temperature oxidizing environments, possessing high electrical conduction and low leakage current.

In this study, BST films were deposited onto Pt/Ti/SiO_2/Si substrates by the sol-gel process and their electrical properties have been investigated. We will also discuss on the evaluation of the thicknesses of the dead layers (DL) interpreted

J. Kim · J. Pak · K. Nam · G. Park (✉)
Department of Physics, Sogang University, Seoul 100-611, South Korea
e-mail: gpark@sogang.ac.kr

from capacitance-voltage (C-V) and current-voltage (I-V) measurements taken in this Au/BST/Pt capacitor.

2 Experiments

The BST solution was purchased from Kojundo chemicals. $Pt/Ti/SiO_2/Si$ substrates were sliced into a size of $20 \times 20\ mm^2$ and degreased using ultrasonic baths following the sequence of acetone, alcohol and DI water for 10 mins each. The films were spin-coated at 2000 rpm for 30 secs and then pyrolysed for 5 mins at the temperature of 350°C . This coating procedure was repeated for 3, 4, 5 and 6 times to obtain BST films with different thicknesses. After coating the films with the desired repetition times, the films were finally annealed in a conventional furnace at temperatures ranging from 600°C to 800°C with a 50°C interval in between.

The crystallographic structures, surface morphology and cross-sectional images of the films were studied using Rigaku D/Max-3C X'-ray diffractometer (XRD) and JEOL JSM-6700F field emission scanning electron microscope (FE-SEM), respectively. XRD data indicates that the BST thin films are polycrystalline with the presence of BST (110), (200) and (211) orientations. The surfaces of these BST films were round and columnar, and a thickness of 320 nm, 380 nm, 460 nm and 560 nm were obtained at the respective coating repetition of 3, 4, 5 and 6 times. It can be estimated that a thickness of roughly 100 nm can be obtained for each coating step.

Circular gold (Au) dots with a diameter of 200 μm were deposited by thermal evaporation using a shadow mask. The C-V and I-V measurements were conducted on these Au/BST/Pt capacitors by HP4194 impedance/gain-phase analyzer and Keithley 617 electrometer, with a micro-manipulating probe station. We evaluated the thickness and dielectric constants of the dead layers using samples treated at 750°C since they showed relatively larger dielectric constants than those treated at lower annealing temperatures and the impurity phases of barium carbonate was observed at 800°C annealed films.

3 Results and discussions

Figure 1 shows the XRD measurements scanned between 2θ angle of 20° and 60° . We have obtained polycrystalline BST films with additional Ti(110), Si(200) and Pt(111) diffraction patterns of the substrates. BST films had (110) and (211) orientations, which increased in intensity with respect to the increase in the substrate temperatures. The impurity phase observed at 800°C annealed samples have been represented by the notation '*' in the graph, and is suspected to be $BaCO_3$

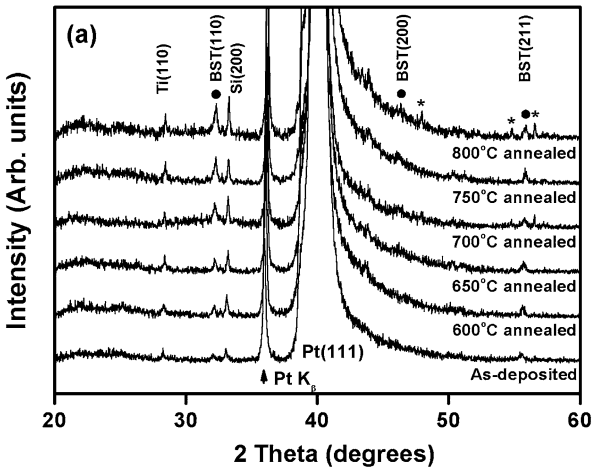

Fig. 1 X-ray diffraction scans between $20 < 2\theta < 60$ degrees of the 320nm thick BST films for the as-deposited and post-annealed films, with the temperature variations given in the right-hand column

that is caused by the reaction of carbon dioxide in air with the undissolved solvent during the annealing procedure [15].

Figure 2 shows the calculated relative dielectric constant of the three-layer coated BST thin films treated at different annealing temperatures, extracted from C-V measurements. The dielectric permittivity increases as the post-annealing temperature rises, which is attributed to increasing grain sizes at higher annealing temperatures. The grains were observed to be round and columnar by surface SEM images, enlarging to an average size of 5, 6 and 7.5 nm at the respective annealing temperatures of 700°C, 750°C and 800°C. Such increase in dielectric constant with respect to grain size has been normally observed in perovskite films.

These films had a thickness difference of about 100 nm for each repetition layers. After thermal evaporating circular Au dots as the top electrode, the electrical properties were

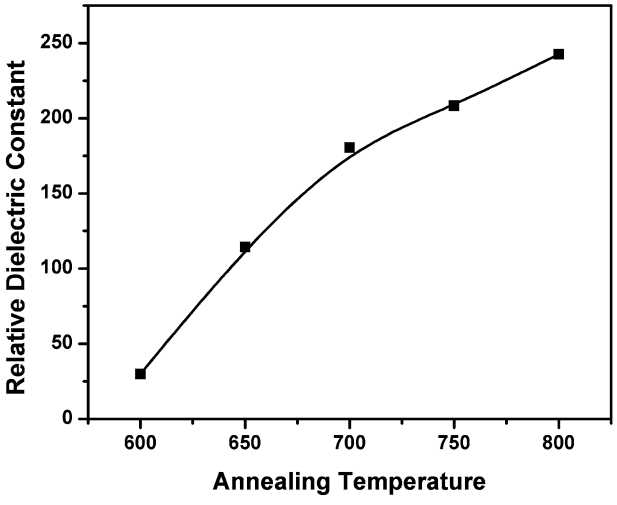

Fig. 2 Calculated relative dielectric constant values with respect to annealing temperatures

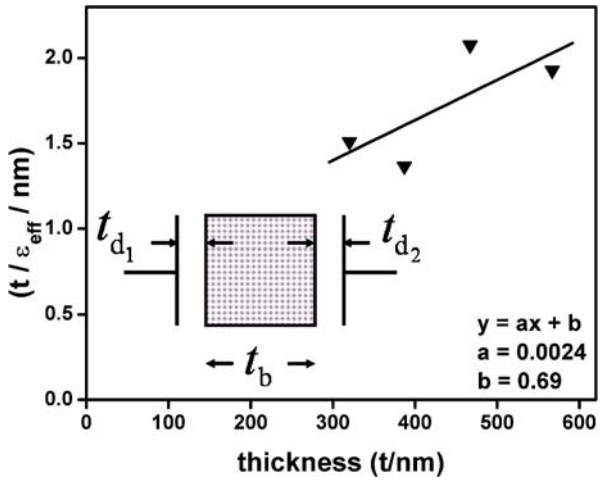

Fig. 3 $t/\varepsilon_{\text{eff}}$ plot as a function of BST thickness t, ranging from 320 nm to 560 nm. The inset shows the schematic diagram of the series capacitor structure formed from the bulk ferroelectric layer (shaded region) and two DLs with thicknesses of t_{d1} and t_{d2}

investigated by an impedance analyzer. As mentioned earlier, the capacitance for these Au/BST/Pt capacitors can be evaluated from the series capacitance model. A brief illustration for the schematic view has been shown in the inset of Fig. 3. Such a series capacitor can be formally expressed by the equation

$$\frac{1}{C_{\text{eff}}} = \frac{1}{C_b} + \frac{1}{C_{d_1}} + \frac{1}{C_{d_2}} \tag{1}$$

where, subscripts b and d refer to the bulk and the dead layer, respectively [14]. The dead layers (DL) d_1 and d_2 represents the DL from Au/BST and Pt/BST interfaces.

According to the phenomenological thermodynamic approach [16], the existence of a DL will induce an interfacial energy per unit area, rather than per unit volume. Therefore, Eq. (1) may be changed into

$$\begin{aligned}\frac{t}{\varepsilon_{\text{eff}}} &= \frac{t_b}{\varepsilon_b} + \frac{t_{d_1}}{\varepsilon_{d_1}} + \frac{t_{d_2}}{\varepsilon_{d_2}} = \frac{t - t_{d_1} - t_{d_2}}{\varepsilon_b} + \frac{t_{d_1}}{\varepsilon_{d_1}} + \frac{t_{d_2}}{\varepsilon_{d_2}} \\ &= \frac{t}{\varepsilon_b} + t_{d_1}\left(\frac{1}{\varepsilon_{d_1}} - \frac{1}{\varepsilon_b}\right) + t_{d_2}\left(\frac{1}{\varepsilon_{d_2}} - \frac{1}{\varepsilon_b}\right)\end{aligned} \tag{2}$$

where, it is usually assumed that $\varepsilon_b \gg \varepsilon_{d1}, \varepsilon_{d2}$ and $t_b \gg t_{d1}$, t_{d2}, giving a linear relationship between $t/\varepsilon_{\text{eff}}$ versus t with a slope of $1/\varepsilon_b$ and a y-axis interception of $t_{d1}/\varepsilon_{d1} + t_{d2}/\varepsilon_{d2}$, as shown in Fig. 3. From these values, ε_b and $t_{d1}/\varepsilon_{d1} + t_{d2}/\varepsilon_{d2}$ were calculated to be 417 and 0.69 nm, respectively. Even though the calculated dielectric constant of the bulk layer was obtained, the thickness of the DL was indistinguishable. Therefore, further measurements on the leakage behavior were conducted to obtain more information on the DL.

The standard Schottky emission equation has been widely used to describe the conduction mechanism in the metal-BST

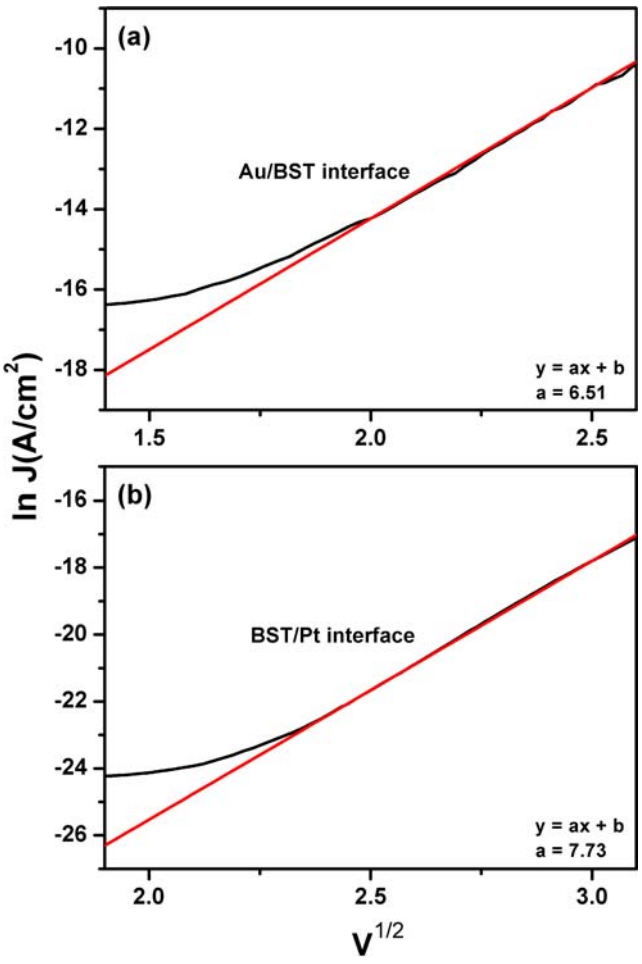

Fig. 4 Leakage current data of Au/BST and Pt/BST interfaces using the modified Schottky emission equation

interface, but it results in improper effective Richardson constant and unphysical relative optical permittivity values [17]. Furthermore, the standard Schottky equation is not applicable to ferroelectric thin films since the mean-free path of ionic mobility in ferroelectric oxides is much less than the thickness [18]. Therefore, the modified Schottky emission equation given in Eq. (3). is preferred,

$$J = A^{**}T^2 \exp\left(-\frac{q\Phi_b}{kT}\right) \exp\left(\frac{q}{kT}\sqrt{\frac{qV}{4\pi\varepsilon_0\varepsilon_r t}}\right) \tag{3}$$

where J is the current density, A^{**} the Richardson constant, T the temperature, $q\Phi_b$ the Schottky barrier height, k the Boltzmann constant, V the applied voltage, ε_0 the permittivity of free space, ε_r the relative dielectric constant, and t the thickness. The linear relation of $\ln(J)$ and $V^{1/2}$ is obtained from the Au/BST interface and BST/Pt interface when the bias voltage is larger than 5 V, as shown in Fig. 4. From these, the values of $t_{d1} \times \varepsilon_{d1} = 50$ nm and $t_{d2} \times \varepsilon_{d2} = 36$ nm can be obtained [19].

Combining data of $t_{d1}/\varepsilon_{d1} + t_{d2}/\varepsilon_{d2} = 0.69$ nm, $t_{d1} \times \varepsilon_{d1}$ = 50 nm and $t_{d2} \times \varepsilon_{d2} = 36$ nm, the DL thickness t_{d1} and t_{d2} were estimated to be less than 6 nm and 5 nm, respectively [20].

4 Conclusion

Ferroelectric BST films were prepared on platinized silicon substrates by the sol-gel process. The films with a thickness of 320 nm were polycrystalline, showing an increase of XRD intensity of the BST peaks with respect to annealing temperatures. $BaCO_3$ peaks observed for 800°C annealed films are resulted from the reaction of the solvent and air. Films treated at 750°C have been coated with different coating layers of 3–6 times. At higher coating layers, the peaks of $BaCO_3$ appeared due to film segregation. The electrical properties were extracted and used for the evaluation of the dead layer thicknesses. With the series capacitance model and modified Schottky emission equation, the thickness of the dead layers for Au/BST and Pt/BST interfaces were calculated to be less than 6 nm and 5 nm, respectively.

Acknowledgments This work was supported by Korea Research Foundation Grant (KRF-2004-005-C00002).

References

1. C.S. Hwang, S.O. Park, H.-J. Cho, C.S. Kang, H.K. Kang, S.I. Lee, and M.Y. Lee, *Appl. Phys. Lett.*, **67**, 2819 (1995).
2. J. Pak, J. Chang, K. Nam, J. Lee, J. Kim, and G. Park, *J. Korean Phys. Soc.*, **42**, S1330 (2003).
3. E. Ko, J. Pak, K. Nam, and G. Park, *J. Korean Phys. Soc.*, **46**, 269 (2005).
4. J.-S. Kim, J.S. Choi, B.H. Park, H.-J. Choi, and J.-K. Lee, *J. Korean Phys. Soc.*, **46**, 183 (2005).
5. S.E. Moon, M.H. Kwak, Y.-T. Kim, H.-C. Ryu, S.-J. Lee, and K.-Y. Kang, *J. Korean Phys. Soc.*, **46**, 273 (2005).
6. Y.H. Wang, B. Gu, G.D. Xu, and Y.Y. Zhu, *Appl. Phys. Lett.*, **84**, 1686 (2004).
7. *Thin Film Ferroelectric Materials and Devices*, edited by R. Ramesh (Kluwer Academic, Boston, 1997).
8. A.K. Tagantsev, V.O. Sherman, K.F. Astefiev, J. Venkatesh, and N. Setter, *J. Electroceram.*, **11**, 5 (2003).
9. A. Von Hippel, NDRC Div., **14**, Rept. 300, PB. 4660 (1944).
10. B.T. Lee and C.S. Hwang, *Appl. Phys. Lett.*, **77**, 124 (2000).
11. C. Zhou and D.M. Newns, *J. Appl. Phys.*, **82**, 3081 (1997).
12. C.S. Hwang, *J. Appl. Phys.*, **92**, 432 (2002).
13. W.Y. Park, K.H. Ahn, and C.S. Hwang, *Appl. Phys. Lett.*, **83**, 4387 (2003).
14. A.M. Bratkovsky and A.P. Levanyuk, *Phys. Rev. Lett.*, **84**, 3177 (2000).
15. M. Viviani, M.T. Buscaglia, P. Nanni, R. Parodi, G. Gemme, and A. Dacca, *J. Eur. Ceram. Soc.*, **19**, 1047 (1999).
16. S.B. Desu, *Mater. Res. Soc. Symp. Proc.*, **541**, 457 (1999).
17. G.W. Dietz, R. Waser, S.K. Steiffer, C. Basceri, and A.I. Kingon, *J. Appl. Phys.*, **82**, 2359 (1997).
18. S. Zafar, R.E. Jones, B. Jiang, B. White, V. Kaushik, and S. Gillespie, *Appl. Phys. Lett.*, **73**, 3533 (1998).
19. B. Chen, H. Yang, J. Miao, L. Zhao, L.X. Cao, B. Xu, X.G. Qiu, and B.R. Zhao, *J. Appl. Phys.*, **97**, 024106 (2005).
20. B. Chen, H. Yang, L. Zhao, J. Miao, B. Xu, X.G. Qiu, B.R. Zhao, X.Y. Qi, and X.F. Duan, *Appl. Phys. Lett.*, **84**, 583 (2004).